Polymer Chemistry

ROYAL SOCIETY OF CHEMISTRY

PAPER

View Article Online
View Journal | View Issue

Check for updates

Cite this: *Polym. Chem.*, 2023, **14**, 3465

Tacticity control approached by electric-field assisted free radical polymerization – the case of sterically hindered monomers†

Wenkang Tu,[a,b,c] Paulina Maksym,[b,d] Katarzyna Chat,[*a,b] Tadeusz Biela,[e] Andrzej Zięba,[f] Kamil Kaminski[a,b] and Karolina Adrjanowicz[*a,b]

Received 2nd May 2023,
Accepted 30th June 2023

DOI: 10.1039/d3py00484h

rsc.li/polymers

We investigate the effect of a high electric field on the free-radical polymerization (FRP) of an acrylate monomer with a large steric hindrance that comes from the isobornyl pendant group. In the presence of static (DC) fields reaching 140 kV cm^{-1}, the polymer product shows reduced dispersity and a remarkable increase in the molecular weight compared to the zero-field reference. Electric-field assisted polymerization of isobornyl acrylate was carried out at 343 K in the presence of 2,2′-azobis(2-methylpropionitrile) (AIBN) as a radical initiator. Surprisingly, pronounced changes were found in the stereochemistry of the obtained polymer. There is an increasing trend for the isotactic triad content with increasing field magnitude. Depending on the reaction conditions, the isotactic triad content (methine carbon region) could be increased from ~16% (0 kV cm^{-1}) up to 36% (140 kV cm^{-1}). By analyzing the temperature dependence of the isotactic to syndiotactic diad ratio, we found that high electric fields increase the contribution of the entropic factor almost three-fold. Our finding provides new opportunities for a simple and versatile stereochemistry control at a level inaccessible so far for conventional radical polymerization.

Introduction

Stereochemistry control (*e.g.*, tacticity or chirality) in radical polymerization is one of the most formidable future challenges in polymer chemistry.[1] While this aspect has been well established by coordination or anionic polymerization, in both conventional free-radical (FRP) and reversible-deactivated radical (RDRP) approaches, tacticity control still remains a non-trivial problem. This is a consequence of the nature of radicals, which, due to the lack of an asymmetric environment around planar carbon radicals, results in non-stereoselective chain propagation. There have been attempts to push forward stereocontrol in radical polymerization by using particular solvents or additives (*e.g.*, fluoroalcohols, Lewis acids, and chiral agents/initiators) that change the local conditions around the radical species.[2–10] However, none of that has ever reached the high level of polymer stereochemical control known from ionic or coordination methods in which metal-based initiators or catalysts are used to generate counter cationic or anionic species at the end of the growing chain. Concerning versatility, sustainability, and production cost, recent stereoregulation approaches compiled with a demand for more complex macromolecular architectures and tailor-made molecular weights and dispersities remain challenging to implement.

Luckily, great support for modern polymerization protocols might come from the benignity of nature providing physical stimuli such as light, ultrasound, microwaves, pressure, geometrical restrictions, and electric and magnetic fields.[11–18] Physical stimuli are simple, inexpensive, and environmentally friendly. Light-mediated polymerization is probably the most extensively exploited and effectively incorporated into different polymerization protocols, including tacticity control.[12,19] Effective strategies in controlling the stereochemistry of macromolecules upon radical polymerization also include organized media, so-called inclusion polymerization/soft and hard confined polymerization (micelles, vesicles, liquid crystals, and 2D

[a]*Institute of Physics, University of Silesia, 75 Pulku Piechoty 1, 41-500 Chorzow, Poland. E-mail: kadrjano@us.edu.pl, kchat@us.edu.pl*
[b]*Silesian Center for Education and Interdisciplinary Research (SMCEBI), 75 Pulku Piechoty 1a, 41-500 Chorzow, Poland*
[c]*State Key Laboratory of Metastable Materials Science and Technology, Nano-biotechnology Key Lab of Hebei Province, Applying Chemistry Key Lab of Hebei Province, Heavy Metal Deep-Remediation in Water and Resource Reuse Key Lab of Hebei, Yanshan University, Qinhuangdao, 066004, China*
[d]*Institute of Materials Engineering, University of Silesia, 75 Pulku Piechoty 1a, 41-500 Chorzow, Poland*
[e]*Department of Polymer Chemistry, Centre of Molecular and Macromolecular Studies, Polish Academy of Sciences, Sienkiewicza 112, 90-363 Lodz, Poland*
[f]*Department of Organic Chemistry, School of Pharmacy with the Division of Laboratory Medicine in Sosnowiec, Medical University of Silesia in Katowice, ul. Jagiellońska 4, 41-200 Sosnowiec, Poland*

†Electronic supplementary information (ESI) available. See DOI: https://doi.org/10.1039/d3py00484h

mesoporous materials).[20,21] Literature findings also demonstrate that physical stimuli might profoundly affect polymerization kinetics and the polymer product macrostructure. For example, high-pressure-assisted or hard-confined reversible deactivation radical polymerization enables overcoming thermodynamic limitations making it possible to obtain polymers with very high molecular weights (M_n) and low dispersities ($Đ$) in a reasonable timeframe. At the same time, externally triggered FRPs have improved reaction control compared to conventional FRPs (even with linear growth of M_n with conversion), giving easy access to polymers with very high M_n and moderate $Đ$.[15,22,23]

We have recently demonstrated that the available pool of external stimuli successfully incorporated into FRP protocols can be enriched by using a high electric field, *i.e.*, an external electric field with field magnitudes $\gg$10 kV cm^{-1}.[24] Thanks to our robust methodology, we produced polymethacrylates of very high M_n and low to moderate $Đ$. It is worth noting that the reaction conditions were as simple as possible. FRPs were carried out in bulk, *i.e.*, without using a solvent or any auxiliary control agents (only monomer + thermoinitiator acting as a radical source). Interestingly, by changing the frequencies and magnitudes of the applied AC/DC electric fields, we have modified the tacticity of the resulting poly(methyl methacrylate)s (PMMAs), at the level inaccessible for FRP.[24] Note that the effect of the external electric field is less explored compared to other physical stimuli, though it has enormous potential to affect the polymerization outcome.[24–26]

Encouraged by these extremely promising findings, we demonstrate the great potential of using an external electric field to support the FRP of a far more challenging monomer. The monomer selected for this study is isobornyl acrylate (IBA), with a 5–6 bicyclic saturated carbon side group that largely hindered the propagation and termination rates of IBA compared to other acrylate monomers (see Fig. 1). A bulky pendant isobornyl group provides rigidity, hardness, good thermal stability, and mechanical properties to the obtained polymer. Although IBA is not a particularly commonly used acrylate monomer, we have chosen it for the present study because of its large bulkiness. Our main goal was to check whether electric-field assisted FRP of IBA would be as effective in increasing control over the reaction as in the case of less sterically hindered methacrylates. We also aim to verify if the external electric field is still in power to change the isotacticity of the produced poly(isobornyl acrylate)s (PIBAs). For that purpose, we carried out FRP of IBA in the presence of a DC electric field of different magnitudes, up to 140 kV cm^{-1} (bulk, 343 K, AIBN as a thermoinitiator). The ongoing FRPs were monitored *via* the dielectric technique. In turn, the resulting PIBA products were characterized *via* spectroscopic and chromatographic methods (nuclear magnetic resonance (^{13}C NMR and ^{1}H NMR), gel permeation chromatography with multiangle light scattering (MALLS) or low angle light scattering (LALLS), and differential scanning calorimetry (DSC)). We demonstrate that with increasing field magnitude, the $Đ$ of the obtained PIBAs decreases, while its M_n remarkably increases to M_n = 366 kg mol^{-1} (at 140 kV cm^{-1}), which is far beyond that achieved by FRP carried out in the absence of a DC electric field (171.4 kg mol^{-1}). Amazingly, we also found that the field-assisted polymerization of IBA enables us to control the tacticity of the obtained polymers. As a result of some degree of branching induced by the high electric field and changes in the isotacticity content (an increase by 20%), PIBA produced at 140 kV cm^{-1} was characterized by a glass transition temperature (T_g) 5.5 K lower than that obtained at 0 kV cm^{-1} despite the much higher molecular weight. In this work, we also provide evidence for the increase in the isotacticity content of poly(*n*-butyl acrylate) P*n*BA (as an example of less bulky acrylate) and poly(isobornyl methacrylate) PIBMA (corresponding methacrylate) polymerized under high electric fields. Therefore, it appears that electric-field-assisted FRP might be a powerful stereochemistry control strategy. Depending on the permanent dipole moment value and its orientation with respect to the growing polymer chain, it is also compatible with a wide range of monomer families and varying steric barriers.

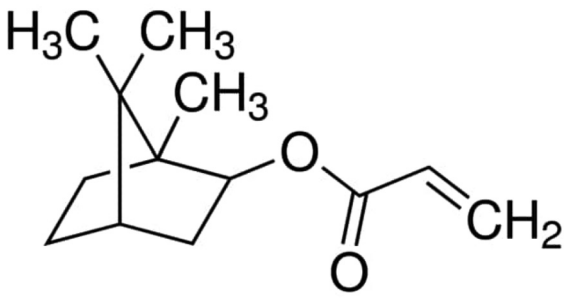

Fig. 1 Chemical structure of IBA.

Experimental section

Materials

Isobornyl acrylate (IBA, 92.7%), methyl acrylate (MA, 99%), 2,2′-azobis(2-methylpropionitrile) (AIBN, 98%), *n*-butyl acrylate (*n*BA, 99%), isobornyl methacrylate (IBMA, 92.5%) and chloroform-*d* ($CDCl_3$, 99.8 atom% D) were purchased from Sigma-Aldrich. Methanol (98%) and chloroform (98.5%) were purchased from Chempur. IBA and MA were purified by passing over a column of activated basic alumina (Sigma-Aldrich) to remove the inhibitors and stored in a fridge. Other reagents were used as received.

Procedures

The polymers were prepared by FRP of a reaction mixture composed of IBA and 0.1 or 0.5 wt% AIBN. The reaction mixture was prepared in a Schlenk flask, degassed by one freeze–pump cycle, and then purged with nitrogen for 20 min. The polymer was precipitated in cold methanol (10-fold excess). The final polymer sample was dried under vacuum to a constant mass, yielding 0.80–1.25 mg pure PIBA. For control experiments, MA,

*n*BA, and IBMA were polymerized in the presence of 0.5 wt% AIBN and purified by precipitation in cold methanol (10-fold excess, yield 0.30–0.40 mg). In that case, the electric-field assisted polymerization conditions were identical to those for IBA.

High-field experiment

Polymerization experiments in the presence and absence of a DC electric field were carried out under isothermal conditions (T = 343 K) for a period of ~4.5 hours with a reaction mixture held in between a plate–plate capacitor (stainless steel electrodes with 20 mm diameter each) separated by a Teflon spacer (thickness: 21 microns). The distance between the electrode was fixed, while the electrode surface was flat and highly polished to maintain a homogeneous electric field. The scheme illustrating reaction conditions can be found in ref. 24 and 26. In each experiment, the capacitor filled with the polymerization mixture was mounted inside a dielectric sample cell and placed inside the temperature control cryostat (liquid nitrogen vapor). DC bias was applied only after reaching the desired polymerization temperature (343 K). The reaction was assumed to be completed when no further changes were observed in the dielectric loss spectra. Then DC bias field was switched off. After each polymerization experiment, the reaction mixtures were removed from the electrodes by dissolving in chloroform-*d* and taken for ^{1}H NMR to obtain [%] conversion. Further characterization of the obtained polymers, such as ^{1}H and ^{13}C NMR, SEC-MALLS/LALLS, and DSC, was performed after evaporating chloroform-*d*, precipitating in cold methanol, and drying to a constant mass.

Dielectric spectroscopy

In this study, we use a dielectric/impedance analyzer (Alpha A-Analyzer) in combination with a high-voltage booster "HVB1000", both from Novocontrol (Germany). The high voltage extension boosts the voltages of the Alpha Analyser up to 500 V (peak voltage). In this configuration, we can cover the frequency range from mHz up to 10 kHz. A high-voltage unit combined with the dielectric spectrometer allows not only the application of a high electric field (AC or DC) to the sample but also measurement of its dielectric response at the same time. The idea is that on top of a sinusoidal voltage of E < 1 kV cm^{-1} – which is typically used for conventional (low-field) dielectric measurements – we apply high DC bias. The DC-field magnitudes reached in this study were as high as 140 kV cm^{-1}. The reaction kinetics is determined by analyzing the ongoing changes in the complex dielectric permittivity, $\varepsilon^* = \varepsilon' - i\varepsilon''$, with time. Dielectric spectroscopy was also used to characterize segmental dynamics of the obtained PIBA samples (conventional low-field measurements, E < 1 kV cm^{-1}). For that, we have also used plate–plate geometry, as described above. Before that, the polymer was purified from the residual impurities and remaining monomers. In all experiments, a Novocontrol Quatro system was used to control the temperature of the sample cell, with stability at 0.1 K. The dielectric spectra recorded upon isothermal polymerization measurements (343 K) were in the frequency range from 0.7 Hz to 10^4 Hz every 100 seconds, while non-isothermal measurements were carried out on purified polymers within 0.09 Hz to 10^6 Hz and a temperature range from 343 K to 393 K (upon heating).

DSC measurements

The calorimetric study was performed using a Mettler-Toledo DSC 1STARe system. The instrument has an HSS8 ceramic sensor with 120 thermocouples and a liquid nitrogen cooling station. Zinc and indium standards were used to calibrate the devices before the measurements. Samples (1.2 mg) sealed in an aluminum crucible (40 μL) were measured at a 10 K min^{-1} fixed heating rate. DSC thermograms were recorded in the temperature range from 293 K to 393 K. The glass transition temperature T_g was determined as the midpoint of the heat capacity increment. The DSC scans for polymers obtained at 0 kV cm^{-1} and 60 kV cm^{-1} were repeated three times with similar results. We observed that the value of the glass transition temperature remains constant, which means that the polymers are thermally stable when heated up to 393 K. The DSC experiment was performed after separating the polymerization product from the remaining mixture.

NMR measurements

Proton nuclear magnetic resonance (^{1}H NMR) spectra were recorded using a Bruker Ascend 600 spectrometer operating at 600 MHz in chloroform as a solvent. Standard experimental conditions and a standard Bruker program were used. The IBA conversions were calculated by integrating the vinyl protons at 6.32 ppm (CH_2=C, monomer) and 5.78 ppm (CH_2=C, monomer) against the methine proton in the polyacrylate backbone of the polymer at 2.11 ppm (–CH–C=O–O) (see Fig. 5). The content of triads for polyacrylates and polymethacrylates has been calculated by quantitative ^{13}C NMR using methine carbon or the carbonyl carbon regions, respectively, based on the previous literature reports.[27,28] The ^{1}H and ^{13}C NMR spectra and peak assignments of PIBAs are presented in the ESI.†

SEC measurements

Absolute molecular weights (M_n) and dispersities ($Đ$) of PIBAs and PIBMAs were measured using a size exclusion chromatography (SEC) system equipped with an 1100 Agilent isocratic pump. ASTRA 4.90.07 8 software (Wyatt Technology Corporation) was used for data collection and processing. Two PLGel 5 μm MIXD-C columns were used for separation. Samples were injected as a solution in methylene chloride at room temperature with a flow rate of 0.8 mL min^{-1}. Molecular weights (M_n) and dispersities ($Đ$) of the produced PMAs and P*n*BAs were determined using a size exclusion chromatography (SEC) system with a Viscotec GPC Max VR 2001 and a Viscotec TDA 305 triple detection containing refractometer, viscosimeter, and low-angle laser light scattering. OmniSec 5.12 was used for data processing. Two D6000M (General Mixed Org 300 × 8 mm) and Dguard (Org Guard Col 10 × 4.6 mm)

columns were used for separation. The measurements were carried out in DMF with LiBr (10 mmol) as the eluent at 40 °C with a flow rate of 0.7 mL min^{-1}.

Results

Following polymerization progress by dielectric spectroscopy

In this work, dielectric spectroscopy was used to investigate polymerization progress in the presence and absence of a static (DC) electric field. Initially, we carried out thermally-initiated IBA FRP in the presence of 0.5 wt% AIBN thermoinitiator. To verify the effect of the initiator's concentration on the properties of the obtained polymer product, we have also carried out the electric field-assisted polymerization of IBA using 0.1 wt% AIBN. For the sake of clarity, the results of the dielectric investigation are presented only for the reaction mixture containing IBA + 0.5 wt% AIBN. The system was maintained at temperature T = 343 K, and a DC electric field of various intensities (60 kV cm^{-1}, 140 kV cm^{-1}) was applied. Fig. 2 shows the representative time evolution of the real (panel (a), (c), (e)) and imaginary (panel (b), (d), (f)) parts of the complex dielectric permittivity recorded in the presence and absence of a DC bias (60 kV cm^{-1} and 140 kV cm^{-1}). In the dielectric spectra of the real part of complex dielectric permittivity (panel (a), (c), (e)), two regions are observed. At lower frequencies, a region with a sharp increase of ε' values was attributed to electrode polarization. This effect is due to the accumulation of ions at the sample–electrode interface.

In turn, at high frequencies, in ε' spectra, a plateau related to the static permittivity of the system is observed. In turn, at the early stages of the reaction, in the dielectric loss spectra (panels (b), (d), (f)), mainly dc conductivity related to the charge transport is seen. With time, it shifts towards lower frequencies, reflecting an increase in the viscosity of the system due to the formation of higher molecular weight polymers. Then, at some point, a relaxation process related to segmental mobility enters the experimental window. It moves toward lower frequencies indicating a slowing down of the polymer dynamics as it approaches the glass transition. The reaction was assumed to be almost completed when significant changes were not observed in the dielectric response as a function of time. This takes approximately 4.5 h.

In Fig. 3a, we present the time-dependent changes in the real part of the complex dielectric permittivity recorded during FRP of IBA with 0.5 wt% AIBN under zero-field conditions and in the presence of DC bias E = 60 kV cm^{-1} and E = 140 kV cm^{-1}. The data were compared for one selected frequency

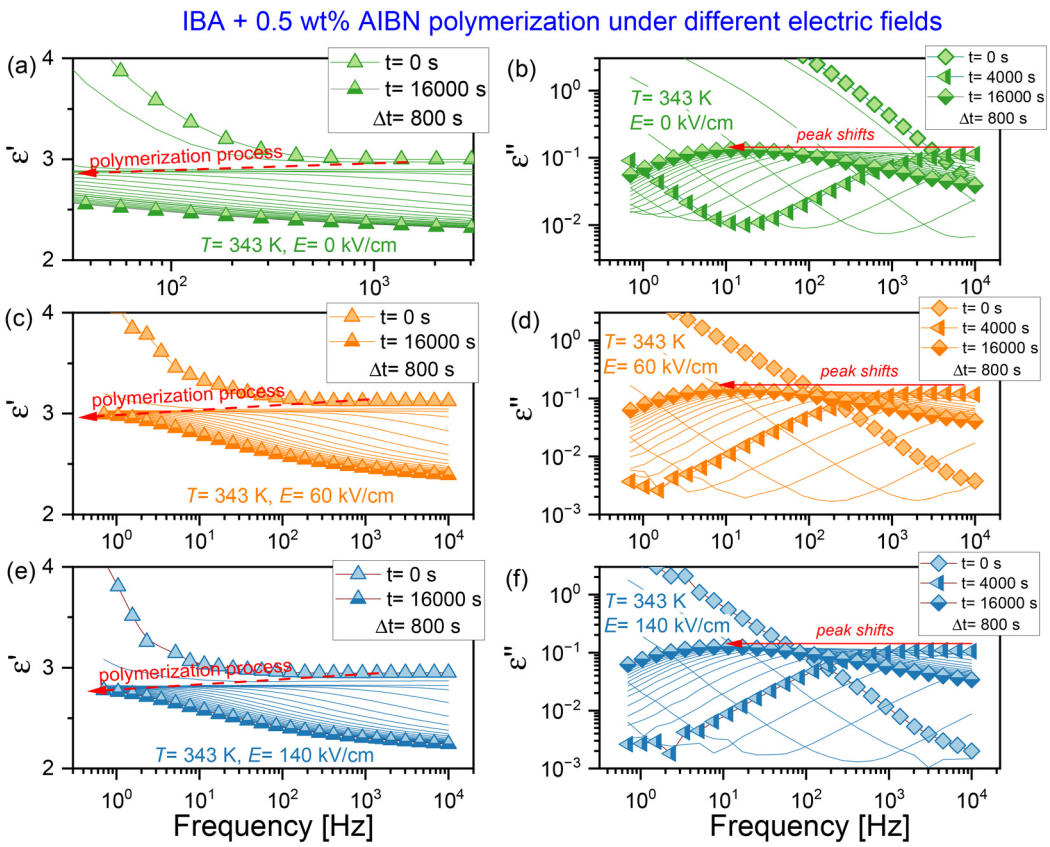

Fig. 2 Representative time evolution of the real (panel (a), (c), (e)) and the imaginary (panel (b), (d), (f)) parts of the complex dielectric permittivity, recorded during isothermal polymerization of IBA with 0.5 wt% AIBN at T = 343 K under no electric field (reference) (panel (a) and (b)) as well as under static (DC) electric fields of E = 60 kV cm^{-1} (panel (c) and (d)) and E = 140 kV cm^{-1} (panel (e) and (f)).

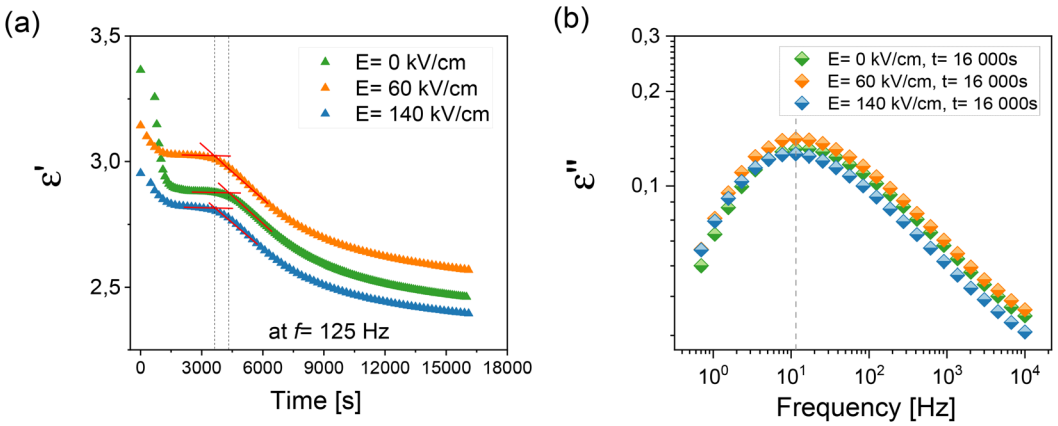

Fig. 3 (a) Time evolution of the real part of the complex dielectric permittivity measured at f = 125 Hz upon FRP of IBA (with 0.5% AIBN) under DC electric field conditions (0 kV cm^{-1}, 60 kV cm^{-1}, 140 kV cm^{-1}). (b) Comparison of the position of the α-loss peak recorded at the very late reaction stage.

(f = 125 Hz). As shown, ε' decreases with time and almost saturates due to viscosity increase which hampers the progress of the reaction. This happens after approximately ~4.5 hours s. As can be seen, the presence of an electric field does not significantly affect the overall reaction time. In turn, Fig. 3b compares the dielectric loss spectra collected at the very final stages of the reaction progress. The position of the α-loss peak is about the same for samples synthesized in the presence and absence of a high electric field. However, it is worth noting that the dielectric data presented in Fig. 3b do not represent a pure polymer response, as they were collected just before purification, evaluating the degree of monomer conversion.

The properties of polymers obtained by field-assisted FRP

In the next step, the obtained PIBAs were purified and isolated by multi-step precipitation. All samples were characterized by NMR spectroscopy and SEC-MALLS. Fig. 4 and Table 1 present the characteristic properties of the obtained PIBAs. Interestingly, as shown in Table 1 and Fig. 4a, the monomer consumption increases with increasing magnitude of the applied electric field from a_{NMR} = 75.5% at zero-field (Table 1, entry 1), through a_{NMR} = 78.9% at E = 60 kV cm^{-1} (Table 1, entry 2), up to a_{NMR} = 84.6% at E = 140 kV cm^{-1} (Table 1, entry 3), which we assume to be the maximum IBA conversion reached under these polymerization conditions. At this point, it is worth mentioning that we have previously reported a decrease in monomer conversion with an increase in the field amplitude for the electric field-assisted FRP of HEMA.[26] On the other hand, in the case of FRP of MMA carried out in the presence of a high electric field, we did not observe that the field magnitude significantly influences the degree of monomer conversion.[24] This suggests that the effect of the external electric field on the degree of polymerization cannot be generalized. It seems that it rather depends on the specific monomer unit used.

Fig. 4b presents SEC-MALLS traces of all produced PIBAs. Using a MALLS (multi-angle laser light scattering) detector

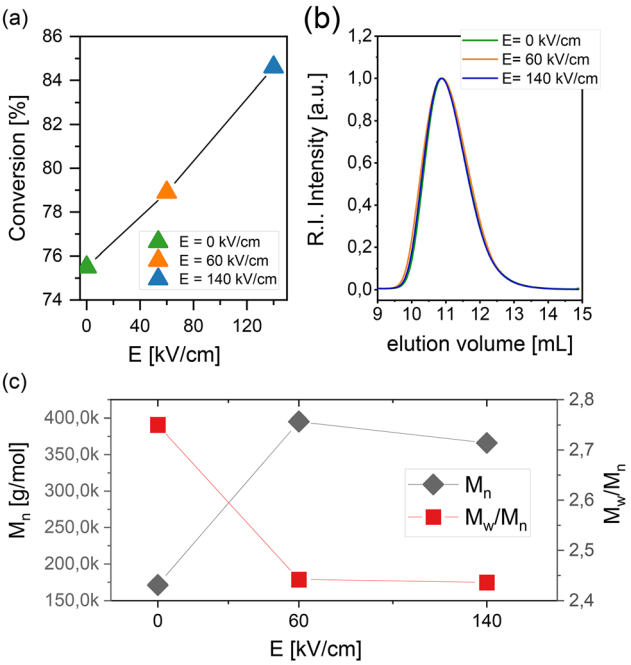

Fig. 4 (a) Monomer conversion plotted as a function of the DC field magnitude. Data were determined based on ^{1}H NMR spectra of the final PIBA samples obtained by high-field polymerization experiments (with 0.5% AIBN). (b) SEC-MALLS traces of PIBA prepared *via* FRP in the presence of external electric fields (0 kV cm^{-1}, 60 kV cm^{-1}, 140 kV cm^{-1}). (c) Changes of M_n and $Đ$ plotted as a function of the field magnitude.

allowed us to determine the absolute molecular weight of the obtained polymers. Although recorded chromatograms are almost indistinguishable at first sight, one should remember that SEC chromatography separates polymers based on their hydrodynamic volume rather than their molecular weight. The hydrodynamic volume of polymers is a complex function of their molecular weight, structure/architecture, solvency, *etc.* Thus, polymers with different molecular weights and architec-

Table 1 Characteristics of PIBA produced by FRP with and without the presence of a high electrical field

No.	Reaction mixture	Electric field intensities [kV cm^{-1}]	Reaction durations [h]	Temperature [K]	Conversion α_{NMR} [a] [%]	PIBA properties			
						M_n [b] [g mol^{-1}]	M_w [g mol^{-1}]	$Đ$ [b]	dn/dc
1	IBA + 0.5 wt% AIBN	0	~4.5	343	75.5	171 400	471 300	2.750	0.1150
2	IBA + 0.5 wt% AIBN	60	~4.5	343	78.9	395 200	965 200	2.442	0.0830
3	IBA + 0.5 wt% AIBN	140	~4.5	343	84.6	366 000	901 500	2.463	0.0830
4	IBA + 0.1 wt% AIBN	0	~19.5	343	83.3	280 100	676 600	2.416	0.0830
5	IBA + 0.1 wt% AIBN	140	~19.5	343	85.6	324 475	713 850	2.200	0.0130

[a] Determined by ^{1}H NMR ($CDCl_3$, 600 MHz). [b] Determined by SEC-MALLS (DCM as eluent).

tures may have the same or similar hydrodynamic volumes. This refers exactly to the case of PIBA. It is also worth emphasizing that traces of obtained samples reveal monomodal shapes with some tailing at lower M_n values regardless of the absence or presence of a high DC electric field. These results are in line with the relatively high $Đ$ = 2.44–2.75 (see Table 1, entries 1–3), reflecting lower homogeneity of the growing chains. However, a five-fold reduction in the initial AIBN concentration leads to slightly better process control at 140 kV cm^{-1}, as evidenced by a lower $Đ$ = 2.2 (see Table 1, entry 5). At this point, it should be clearly stated that electric field-assisted FRP of IBA was a less controlled process than those previously reported for MMA and HEMA, which were carried out under similar conditions (bulk, 0.5 wt% AIBN). On the other hand, one should bear in mind that FRP of IBA similar to other acrylate monomers, might often be accompanied by the occurrence of unwanted side reactions such as (i) intramolecular chain transfer (*i.e.*, backbiting), (ii) βC-scission reactions and (iii) intermolecular chain transfer.[29–31] Notably, backbiting and βC-scission side reactions can slow down the polymerization process, shortening the length of the main chain and producing macromonomers. However, the electron paramagnetic resonance (EPR) measurements have revealed that these reactions are expected to become important at elevated temperatures.[32] Thus, to avoid/minimize unwanted side reactions, we carried out our experiments at a much lower temperature (343 K) and without using any solvent. The structure of the obtained PIBA products was confirmed based on ^{13}C NMR spectra, in which signals from vinyl groups (that could be derived from macromonomers) were not visible. At this point, it needs to be mentioned that IBA can be controllably polymerized by RDRPs in the temperature range of 323–363 K with avoidance of unwanted side reactions.[33–36] However, reported polymers were characterized by $M_n \leq 100$ kg mol^{-1} with variable conversion.[33–37] On the other hand, the emulsion polymerization presented by Back and Schork allows obtaining PIBA samples with a molecular weight of around 1000 kg mol^{-1}.[38]

In the next step, we have also attempted to determine the branching of PIBA. Unfortunately, because the obtained polymers were highly polydisperse, we could not determine branching in a classical way, *i.e.*, from the radius of gyration. Nevertheless, we have extracted some valuable information about it by analyzing the relationship between molecular weight and elution volume (corresponding to changes in the hydrodynamic volume). The obtained relationship between the molar mass of produced polymers and the elution volume can be found in the ESI.† From that analysis, we found that the increase in the DC field magnitude results in obtaining polymers with higher molecular weights. However, within the same hydrodynamic volume, they are more tightly packed, meaning that there is certainly some degree of branching induced by a high electric field. Branch polymers are more compact and might have the same hydrodynamic volume as linear or less branched polymers with lower molecular weights. So, the same hydrodynamic volume translates into an identical elution volume but not essentially the same molecular weight.

In the next step, we aimed to verify if the steric hindrance factor might be responsible for less control over the reaction. For that purpose, two control experiments were performed using methyl acrylate and *n*-butyl acrylate, which are less bulky monomers compared to IBA. Electric field-assisted polymerization of MA was carried out at 0 kV cm^{-1} and 65 kV cm^{-1}, while maintaining a constant temperature of 343 K (0.5 wt% AIBN). The experimental conditions for *n*BA were similar, except that we used higher DC field magnitudes, *i.e.* 140 kV cm^{-1}. SEC-LALLS traces of produced PMAs and structure confirmation by ^{1}H and ^{13}C NMR analysis are given in the ESI.† Surprisingly, in that case, we have observed a much better control over MA FRPs than over IBA, both in the presence and the absence of the DC e-field. More interestingly, poly(methyl acrylate) PMA produced at 65 kV cm^{-1} reveals that $Đ$ = 1.42, which is much lower than that obtained at 0 kV cm^{-1} ($Đ$ = 1.70). At the same time, it is comparable to values reported previously for PMMAs obtained in the presence of the DC field. SEC-LALLS traces of PMA samples obtained at 0 kV cm^{-1} and 65 kV cm^{-1} also revealed more symmetric shapes with lower tailing at low M_n (see the ESI†). The dispersity of P*n*BA (being bulkier than MA but still not as sterically hindered as IBA) synthesized at 140 kV cm^{-1} is $Đ$ = 1.97, that is, in between the values reported for MA and IBA. Therefore, we can indeed presume that the presence of a sterically hindered side group affects the dispersity of polymers produced under high electric fields. On the other hand, the results recorded for P*n*BA confirm the same trend in M_n values as observed for other

acrylates; namely, the molecular weight of produced polymers increases with increasing field magnitude (M_n = 2 870 000 g mol^{-1} at 0 kV cm^{-1}, and M_n = 3 820 000 g mol^{-1} at 140 kV cm^{-1}, see the ESI† for SEC traces).

The results presented in Fig. 4c and Table 1 demonstrate that the increase in the amplitude of the applied electric field is accompanied by an increase in M_n and a decrease in $Đ$ of the obtained PIBAs. Similar findings were also reported for other acrylates, such as PMAs and *n*BAs. On the other hand, in the case of the field-assisted FRP of PMMA and PHEMA M_n was found to decrease with increasing field magnitude.[24,26] At the moment, we cannot provide a defined explanation of this finding. For that, more studies are needed for testing monomers from different families. We assume that several factors could be responsible for such results. This might possibly include the difference between the reactivity of acrylates and methacrylates related to the stability of radicals. Note that acrylates form secondary radicals as the propagating end group, while methacrylates form more stable tertiary ones. The stability of the tertiary radical is thought to lower the reactivity of the propagating end for further polymerization.[39] Apart from that steric effects, the dipole moment value of the monomer unit and its location with respect to the growing polymer chain, or the importance of the secondary reactions might contribute to the final M_n of the produced polymer.

In Fig. 5, we compare conversion *versus* time and the corresponding semi-logarithmic plot obtained for polymerization experiments carried out in the presence and absence of a high electric field. As can be seen, conversion and changes of the monomer concentration (analyzed as $\ln[M]_t/[M]_0$) with time show similar evolution for 0 kV cm^{-1} and 140 kV cm^{-1}. Nevertheless, to analyze in more detail the kinetics aspects of electric-field assisted polymerization more detailed studies are needed in the future.[40]

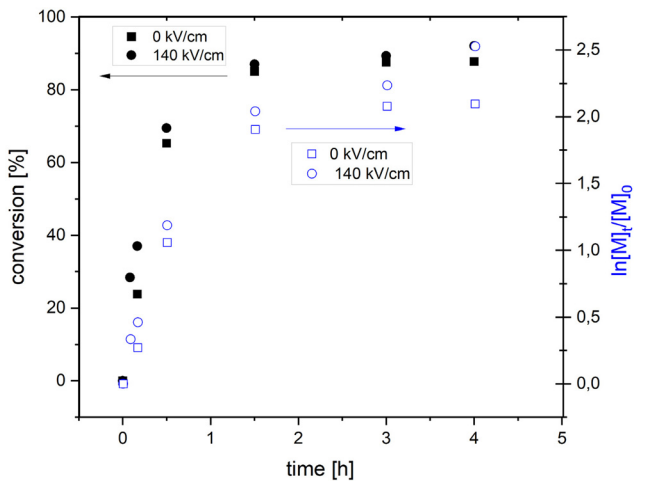

Fig. 5 Conversion *versus* time and corresponding semi-logarithmic plot obtained for FRP of IBA carried out at 343 K in the presence and absence of high electric fields (140 kV cm^{-1} and 0 kV cm^{-1}).

As a next step, we have also analyzed the effect of a high electric field on the stereoregularity of the obtained PIBA samples. The motivation for this investigation was our previous finding showing that the tacticity of PMMA can be modified during the FRP by applying an electric field. In that case, we have also found that increasing the DC field magnitude leads to polymers with a higher isotacticity content.[24] Therefore, to evaluate the PIBA microstructure, we have analyzed samples obtained in the presence of 0.5 wt% AIBN at 0 kV cm^{-1} and 140 kV cm^{-1} using ^{13}C NMR. It is worth noting that previously the configurational sequence of PIBA had been thoroughly determined by one-dimensional [^{1}H, ^{13}C{^{1}H}] and two-dimensional (HSQC, TOCSY and HMBC) NMR spectra.[27,28] Based on that, we have calculated the *mm*/*mr*/*rm*/*rr* triad content assignment to the methine carbon region from 40.5 to 42.5 ppm. The proportions of isotactic, syndiotactic and atactic triads in PIBAs obtained at 0 and 140 kV cm^{-1} are presented in Fig. 6a, while the expanded backbone methine carbon regions for these samples are shown in Fig. 6b. As shown, the content of isotactic triads in PIBA samples increases by 20% when the field magnitude is increased to 140 kV cm^{-1}. These results align with our previous observations reported for MMA polymerization under a DC electric field.[24] Considering the difficulties associated with tacticity control in FRP, our methodology is an excellent alternative to conventional time- and energy-consuming chemical routes enabling fine-tuning polymer stereochemistry. It is as simple as possible, does not require any solvents, expensive reagents, or multi-steps, and, more importantly, can be easily adapted to various monomers. At the current stage of our investigation, we cannot provide a definite explanation for the features of the growing polymer chain, making it more prompt for isotacticity control by the electric field, and how far we can go with that. As we suppose, this might depend on the polarity of the monomer unit since the value of the dipole moment determines how easily it can align along the field lines, or either a particular alignment/orientation of the dipole moment with respect to the propagating chain.

The influence of a high electric field on tacticity is not limited only to FRP of MMA, HEMA, or IBA. In our opinion, it is a more general finding observed not only for methacrylates and acrylates but possibly also for styrene-based monomers or even (meth)acrylamides. However, investigating that aspect is certainly far beyond the main scope of this paper and needs a proper investigation in the future. Nonetheless, to enhance the significance of our finding, we have additionally performed electric field-assisted FRP of *n*-butyl acrylate (*n*BA) and isobornyl methacrylate (IBMA). The chemical structure of both monomers can be seen in Fig. 7. We have chosen IBMA to directly compare with IBA (methacrylate *vs.* acrylate with the same large steric hindrance). In turn, *n*BA provides a less bulky side group compared to IBA (less bulky *vs.* more bulky polyacrylate).

Table 2 tabulates fractions of isotactic, syndiotactic, and atactic triads – as determined by ^{13}C NMR – of PIMBA, PIBA,

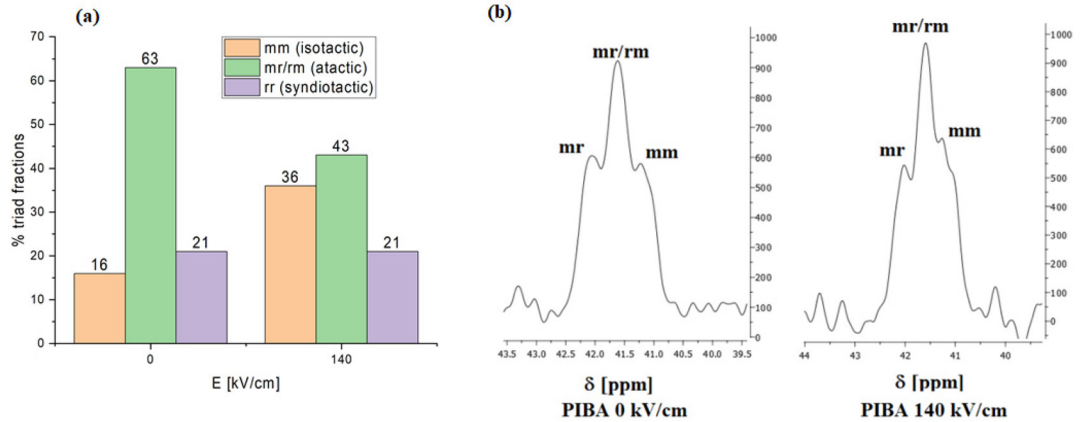

Fig. 6 (a) Triad fraction [%] of methine carbon regions in PIBA estimated *via* ^{13}C NMR spectroscopy as demonstrated in panel (b). Data were collected for five samples obtained by polymerization of IBA in the presence of 0.5 wt% AIBN at T = 343 K at zero field and in the presence of the DC fields (140 kV cm^{-1}).

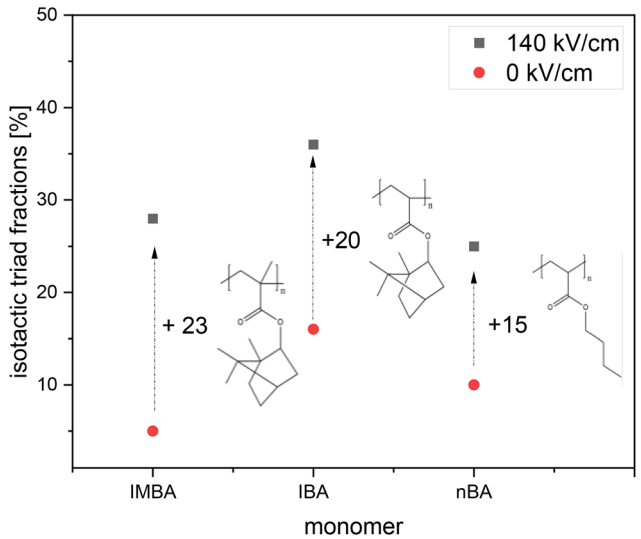

Fig. 7 Changes in the isotacticity content resulted from the DC field effect upon FRP polymerization of IMBA, IBA, and *n*BA at 343 K.

Table 2 Characteristic changes in the tacticity of PIBMA, PIBA, and P*n*BA synthesized by electric-field assisted FRP

Monomer	Triad fractions [%]	DC field magnitude 0 kV cm^{-1}	DC field magnitude 140 kV cm^{-1}	Dipole moment[c]
IMBA[a]	*rr*	40	44	1.85 D
	mr	55	28	
	mm	5	28	
IBA[b]	*rr*	21	21	2.37 D
	mr	63	43	
	mm	16	36	
*n*BA[b]	*rr*	27	4	2.40 D
	mr	63	71	
	mm	10	25	

[a] Determined from the carbonyl carbon region in ^{13}C NMR based on ref. 41. [b] Determined from the methine carbon region in ^{13}C NMR based on ref. 42. [c] Taken from the ref. 40.

and P*n*BA samples obtained by electric field-assisted FRP. Polymerization conditions were identical for each monomer (T = 343 K, 0.5 wt% AIBN). Polymerization experiments were carried out at 0 kV cm^{-1} and 140 kV cm^{-1}. The results indicate that in the presence of a DC field, isotacticity content increases, but the outcome depends on the specific monomer used. This is visualized better in Fig. 7.

Junkers *et al.* recently published a paper providing dipole moment values for different polyacrylates and polymethacrylates.[40] For IBA, IMBA, and *n*BA they report 2.37 D, 1.85 D, and 2.40 D, respectively. When comparing these values with differences in the isotacticity content produced by high e-fields, one can note that IBA and *n*BA – of comparable dipole moment values but different bulkiness of the side group – show a pronounced difference in the isotactic fraction (20% for PIBA and 15% for P*n*BA). In turn, for IBMA (1.85 D) – with a dipole moment much lower than IBA but having the same steric hindrance – changes in the isotacticity content are somehow comparable to PIBA (23% for PIBMA, 20% for PIBA). Notably, *n*BA, less bulky among the other monomers, exhibits the lowest increase in isotacticity. Considering this, we suppose that significant steric hindrance might contribute to an increase in the isotactic fraction. The value of the net dipole moment is undoubtedly an important parameter, as much as its orientation with respect to the growing polymer chain.

To provide deeper insight into tacticity changes induced by a high electric field, we have performed additional measurements which employ the absolute reaction theory. Our focus was to recognize whether syndiospecific propagation under high electric fields is predominantly controlled by the entropic or enthalpic factor. In order to achieve this, FRP of IBA (with 0.5 wt% AIBN) was performed under 0 kV cm^{-1} and 140 kV cm^{-1} at four different temperatures (328 K, 333 K, 338 K, and 348 K). At each temperature, the fractions of *mm*, *mr*, and *rr*

Table 3 Values estimated based on the absolute reaction rate theory

DC field magnitude	T [K]	*mm*	*mr*	*rr*	$\Delta H^{i}_{act} - \Delta H^{s}_{act}$, [kJ mol^{-1}]	$\Delta S^{i}_{act} - \Delta S^{s}_{act}$, [J mol^{-1} K^{-1}]	Bernoullian model (0th-order Markov) $P(m)/P(r)$[a]	1st-order Markov $P(m/r)$[b]	1st-order Markov $P(r/m)$[c]
0 kV cm^{-1}	328	9	65	26	2.07 ± 0.30	5.92 ± 0.97	0.71	0.88	0.88
	333	11	62	27			0.72	0.86	0.86
	338	17	56	27			0.82	0.83	0.83
	348	26	48	26			1.00	0.79	0.79
140 kV cm^{-1}	328	22	39	39	5.10 ± 0.54	15.21 ± 1.62	0.71	0.47	0.47
	333	27	40	33			0.89	0.43	0.44
	338	35	41	24			1.25	0.37	0.41
	348	43	40	17			1.70	0.31	0.37

[a] Where $P(m) = mm/(mm + mr + rr)$ and $P(r) = rr/(mm + mr + rr)$ and $P(m)/P(r) = P(m)/(1 - P(m))$. [b] Estimated from following equation: $P(m/r) = (mr)/[2(mm) + (mr)]$. [c] Estimated from following equation: $P(r/m) = (mr)/[2(rr) + (mr)]$.

triads were analyzed in the synthesized polymers based on ^{13}C NMR. The results are tabulated in Table 3. According to the absolute reaction rate theory, the ratio between meso (P_m) and racemic diads (P_r) can be related to the corresponding differences in activation enthalpy ($\Delta H^{i}_{act} - H^{s}_{act}$) and activation entropy ($\Delta S^{i}_{act} - S^{s}_{act}$) *via* the following relation

$$\ln\frac{P_m}{P_r} = \frac{\Delta S^{i}_{act} - \Delta S^{s}_{act}}{R} - \frac{\Delta H^{i}_{act} - \Delta H^{s}_{act}}{RT} \quad (1)$$

The P_m/P_r ratio is estimated based on individual triad fractions, *i.e.*, $\frac{P_m}{P_r} = ([mm] + [mr]/2)/([rr] + [mr]/2)$. The temperature dependences of $\ln\frac{P_m}{P_r}$ for PIBA samples synthesized at 0 kV cm^{-1} and 140 kV cm^{-1} are shown in Fig. 8. The data were fitted with linear functions, while the fitting parameters were retained in Table 3.

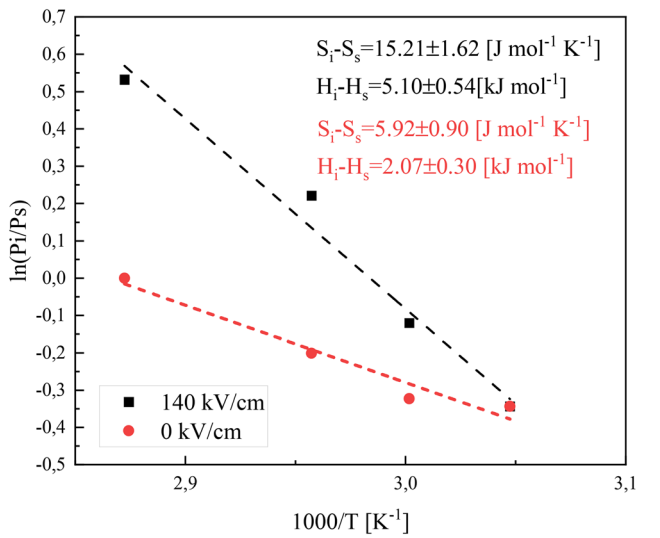

Fig. 8 Temperature dependence of the isotactic to syndiotactic diad ratio for PIBA synthesized *via* free-radical polymerization at 0 kV cm^{-1} and 140 kV cm^{-1}.

The obtained results suggest that a 140 kV cm^{-1} electric field amplifies the differences in activation entropy and activation enthalpy between isotactic and syndiotactic propagations, while the fundamental trends remain analogous. In fact, in both scenarios (with and without the presence of a high electric field), syndiospecific propagation seems to be governed by enthalpic and entropic factors. However, the entropic factor exhibits a more pronounced effect under high e-fields, whereas the enthalpic factor exhibits a more pronounced effect when the field is absent. There is almost a three-fold increase in the contribution coming from the entropic factor under high electric fields. The presence of a high electric field appears to intensify the impact of both enthalpic and entropic factors on the organization of propagating chains, potentially leading to a preference for one tacticity over another (increasing the isotactic fractions as supported by ^{13}C NMR results).

Additionally, we also check if the propagation of the monomer chain fulfills the Bernoulian or 1st order Markov statistics. To assess both models, we have calculated the $P(m)/P(r)$, $P(r/m)$, and $P(m/r)$ ratios. Regarding the Bernoullian model, the first data set, obtained for samples polymerized at 0 kV cm^{-1}, presents a more limited range of $P(m)/P(r)$ values, changing only from 0.71 to 1.00. Conversely, the second data set, derived from polymerization experiments carried out at 140 kV cm^{-1}, exhibits a more expanded range, changing from 0.71 to 1.70. It is essential to note that both data sets do not constitute an optimal fit for the Bernoullian model due to variations in $P(m)/P(r)$ values within each of them. Since the data deviate from unity, the propagation of the monomer chain was described by 1st-order Markov statistics. To confirm the 1st-order Markov model, the sum of $P(m/r)$ and $P(r/m)$ should be approximately 1. As depicted in Table 3, the data corresponding to the FRP of IBA at 0 kV cm^{-1} display a more restricted range of $P(m/r)$ and $P(r/m)$ values (0.79 to 0.88) in comparison to the second set calculated for 140 kV cm^{-1} (0.31 to 0.47 for $P(m/r)$ and 0.37 to 0.47 for $P(r/m)$). This finding indicates that the propagation of the monomer chain at zero field adheres more to the 1st-order Markov statistics, while in the presence of a high electric field it does not.

Dielectric relaxation and calorimetric investigation of the glass transition dynamics of the obtained PIBAs

As a final step of our investigation, we have characterized the glass transition dynamics of produced PIBA samples. For that, dielectric relaxation and calorimetric measurements were performed on purified polymers. Measurements were carried out under low-field conditions (no bias field was applied). Dielectric spectra were collected on heating, and the measurements were carried out in the temperature range of 323 K–393 K. Fig. 9a and b shows the representative dielectric loss spectra for PIBA polymerized at zero-field (panel a) and under the DC filed E = 60 kV cm^{-1} (panel b). For both samples, we observed only the α-relaxation process in the dielectric loss spectra, which shifts toward higher frequencies with increasing temperature indicating a slowing down of the segmental mobility as it approaches the glass transition. The dielectric loss spectra were analyzed using the Havriliak–Negami (HN) function:[43]

$$\varepsilon^*(\varpi) = \varepsilon_\infty + \frac{\Delta\varepsilon}{[1 + (i\varpi\tau_{HN})^{\alpha_{HN}}]^{\gamma_{HN}}} \quad (2)$$

where ε_∞ is the high-frequency limit permittivity, $\Delta\varepsilon$ is the relaxation strength, τ_{HN} is the relaxation time, α_{HN} and γ_{HN} are the parameters characterizing the shape of the dielectric loss curve, while ω is the angular frequency ($\omega = 2\pi f$). Based on fitting parameters, α-relaxation times were determined. Fig. 9c shows the temperature dependence of the α-relaxation times for PIBA samples polymerized at zero-field and in the presence of the DC electric field. As demonstrated, the segmental dynamics of the polymer obtained in the absence of an electric field is slower compared to the sample synthesized under high DC field conditions. The temperature dependences of the α-relaxation times for both tested samples (0 kV cm^{-1} and 60 kV cm^{-1}) were fitted by the Vogel–Fulcher–Tammann (VFT) equation:[44–46]

$$\tau_\alpha = \tau_\infty \exp\left(\frac{D_T T_0}{T-}\right) \quad (3)$$

where τ_∞ is the relaxation time, T_0 is the temperature at which τ_α goes to infinity, and D_T is the fragility parameter. We have determined the glass transition temperature (T_g) for both PIBA samples as a temperature at which τ_α = 10 s. The glass transition temperature is usually defined for τ_α = 100 s. However, to avoid the extrapolation of $\tau_\alpha(T)$ one can also estimate its value using a shorter relaxation time. The glass transition temperature of PIBA synthesized at zero-field is 358.6 K, while for the sample obtained in the presence of the DC e-field T_g is 353.7 K. The fragility parameter, m, which quantifies the seg-

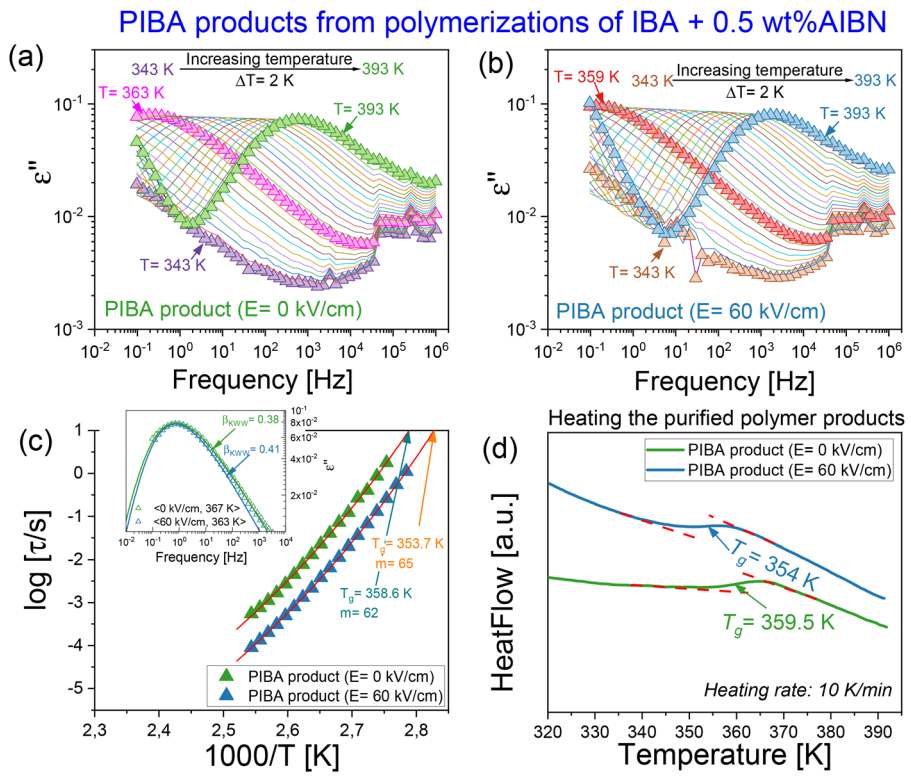

Fig. 9 Dielectric loss spectra measured at different temperatures for PIBA obtained by FRP in the (a) absence and (b) presence of a DC electric field. (b) The temperature dependence of α-relaxation times for the PIBA samples polymerized at zero-field and under high DC fields (60 kV cm^{-1}). The solid lines are the fitting of the data to the VFT equation. The inset shows the comparison of the shape of α-loss peak for PIBA obtained by FRP in the absence and (c) presence of a DC electric field. (d) DSC thermograms for PIBA samples synthesized by free-radical polymerization under high electric fields.

mental relaxation time or any other dynamic variables, such as viscosity or diffusion coefficient, increases as it approaches the glass transition temperature, and was found to be slightly lower for the sample obtained in the presence of a high electric field. Nevertheless, both values, m = 62 (60 kV cm^{-1}) and m = 65 (0 kV cm^{-1}) allow classifying PIBA as a rather strong glass-forming system.[47]

In Fig. 9d, we show the representative DSC thermograms of the obtained PIBAs. An endothermic event observed in both cases is related to the vitrification process. Importantly, in the DSC scans carried out from T = 293 K to T = 393 K we did not notice any crystallization or melting event indicating the eventual semicrystalline character. The T_g values estimated from the DSC data are 359.5 K for PIBA polymerized at zero-field and 354 K for the sample obtained in the presence of the DC field of E = 60 kV cm^{-1}. They agree very well with the dielectric data. On the other hand, T_g values for PIBAs determined in this work are slightly lower than those reported in the literature.[31,33,48,49] This might be related to the differences in the tacticity of the analyzed samples. Moreover, it was also observed that the glass transition temperature of the sample synthesized by FRP supported by the DC field is lower than that obtained under no field conditions. Thus, an increase in the isotacticity of PIBA is accompanied by a reduction of T_g. We have previously demonstrated similar results for PMMA obtained by free radical polymerization carried out either in the presence of AC or DC fields.[24] It is worth noting that the molecular weights of PIBA samples obtained by us are much higher than those reported in the literature. Therefore, as determined by us, the T_g values should not be influenced by the molecular weight effect.[50] At this point, we wish to recall the SEC-MALLS data for PIBA which indicate that the presence of a high electric field induces some degree of branching. A higher degree of branching should generally lower T_g, which might additionally account for the observed differences in T_g values. From the above, we conclude that a combined effect of both factors – tacticity and branching – should be probably taken into account when discussing changes in T_g for acrylates obtained under high electric fields.

We have also compared the distribution of the α-relaxation times for PIBAs obtained in the presence and absence of a high e-field. In the inset of Fig. 9c, we show the dielectric loss spectra for both samples. The data were collected for approximately the same relaxation time. The shape of the α-loss peak is very similar. To describe the distribution of the segmental relaxation, we have used the stretched exponent β_{KWW} from the one-sided Fourier transform of the Kohlrausch and Williams and Watts function (KWW):[51,52]

$$\phi(t) = \exp\left[-\left(\frac{t}{\tau_\alpha}\right)^{\beta_{KWW}}\right] \quad (4)$$

where t is the time and τ_α is the relaxation time. The value of β_{KWW} varies within 0–1 and quantifies the non-exponential character of the relaxation process (β_{KWW} = 1 corresponds to the exponential power law, classical Debye-type relaxation). With broadening the relaxation spectrum, β_{KWW} gets smaller. As demonstrated in the inset of Fig. 9c, the value of the stretching exponent is slightly higher for the PIBA sample obtained by field-assisted FRP, and it is equal to 0.41, while for the polymer synthesized in the absence of a high-electric field β_{KWW} = 0.38. Similar findings have also been reported in our recent work on the effect of isotacticity on the glass transition dynamics of PMMA. In that case, for isotactic-rich PMMA sample segmental relaxation was narrower (β_{KWW} = 0.53) than that for s-PMMA (β_{KWW} = 0.45).[53] This is another argument suggesting higher isotacticity of the polymer recovered from the high electric field-supported polymerization.

Conclusions

Herein, we have employed a high electric field to support the free radical polymerization of the problematic acrylate monomer with a large steric hindrance provided by the isobornyl group. We demonstrate that with the aid of an external electric field, it is possible to overcome thermodynamic limitations and target high M_n polymers with surprisingly good control over the tacticity in FRP. The isotactic content is tuned just by changing the magnitude of the electric field. In contrast to our previous work on methacrylate monomers (MMA and HEMA), here, we found that electric-field assisted FRP of acrylates (IBA, *n*BA and MA) results in the increase of the molecular weight with increasing field magnitude. In addition to that, we also found that the presence of a sterically hindered side group affects the dispersity of polymers produced under high electric fields. A high electric field promotes some degree of branching; therefore for the same hydrodynamic volume, we get more tightly packed PIBA structures.

When it comes to improved control over the properties of the obtained polymers, it probably depends on multiple factors such as steric effects, the value of the dipole moment or the orientation of the net dipole moment with respect to the main chain. We have demonstrated this using IBA, IMBA, and *n*BA. Monomers with comparable dipole moment values but different bulkiness of the side group exhibit a bit different increase in the isotacticity fraction under high fields. For monomers with the same large steric hindrance but not essentially the same dipole moment values, we found comparable changes in the isotacticity content under high electric fields. An interesting finding which comes from this study is also that a high electric field increases the activation enthalpy and the activation entropy for syndiospecific propagation, but definitely the entropic factor is affected more. This might potentially account for the preference of one stereospecificity over the other. At the same time, the determined $\ln(k_p)$ values for IBA indicate that the external electric field has a minimal impact on the polymerization rate.

Summarizing, this work and our recent findings demonstrate the great potential of using a high electric field to affect the molecular weight, dispersity, and tacticity during FRP. Our protocols are simple, highly effective, and easily adapted to

different classes of monomers. Thus, electric field-assisted polymerization emerges as an up-and-coming and facile method complementing the modern polymer chemistry toolbox to obtain stereocontrolled polymers for a large pool of polar monomers in a clean, simple, and inexpensive way.

Conflicts of interest

There are no conflicts to declare.

Acknowledgements

KA and KC are grateful for the financial support from the National Science Centre within the framework of the SONATA BIS project (grant no. 2017/26/E/ST3/00077).

References

1 K. Parkatzidis, H. S. Wang, N. P. Truong and A. Anastasaki, Recent Developments and Future Challenges in Controlled Radical Polymerization: A 2020 Update, *Chem*, 2020, **6**(7), 1575–1588, DOI: 10.1016/j.chempr.2020.06.014.

2 K. Yamada, T. Nakano and Y. Okamoto, Synthesis of Syndiotactic Poly(Vinyl Alcohol) from Fluorine-Containing Vinyl Esters, *Polym. J.*, 1998, **30**(8), 641–645, DOI: 10.1295/polymj.30.641.

3 Z. Wu, C. H. Peng and X. Fu, Tacticity Control Approached by Visible-Light Induced Organocobalt-Mediated Radical Polymerization: The Synthesis of Crystalline Poly(N, N-Dimethylacrylamide) with High Isotacticity, *Polym. Chem.*, 2020, **11**(27), 4387–4395, DOI: 10.1039/D0PY00587H.

4 W. Liu, K. Tang, Y. Guo, Y. Koike and Y. Okamoto, Tacticity Control in the Radical Polymerization of 2,2,2-Trifluoroethyl Methacrylate with Fluoroalcohol, *J. Fluorine Chem.*, 2003, **123**(1), 147–151, DOI: 10.1016/S0022-1139(03)00114-3.

5 W. Liu, Y. Koike and Y. Okamoto, Stereochemistry of the Radical Polymerization of Vinyl Pentafluorobenzoate, *Polymer*, 2004, **45**(16), 5491–5495, DOI: 10.1016/J.POLYMER.2004.06.003.

6 S. H. Shim, M. K. Ham, J. Huh, Y. K. Kwon and Y. J. Kwark, Simultaneous Control over the Molecular Weight and Tacticity of Poly(Vinyl Acetate) Using a Low-Temperature Photoinitiated RAFT Process in Fluoroalcohols, *Polym. Chem.*, 2013, **4**(21), 5449–5455, DOI: 10.1039/C3PY00203A.

7 Y. Isobe, D. Fujioka, S. Habaue and Y. Okamoto, Efficient Lewis Acid-Catalyzed Stereocontrolled Radical Polymerization of Acrylamides, *J. Polym. Sci., Part A: Polym. Chem.*, 2000, **33**(7), 42, DOI: 10.1021/ja015888l.

8 K. Yamada, T. Nakano and Y. Okamoto, Stereospecific Free Radical Polymerization of Vinyl Esters Using Fluoroalcohols as Solvents, *Macromolecules*, 1998, **31**(22), 7598–7605, DOI: 10.1021/MA980889S.

9 K. Satoh and M. Kamigaito, Stereospecific Living Radical Polymerization: Dual Control of Chain Length and Tacticity for Precision Polymer Synthesis, *Chem. Rev.*, 2009, **109**(11), 5120–515610, DOI: 10.1021/cr900115u.

10 J.-F. O. Lutz, D. Neugebauer and K. Matyjaszewski, Stereoblock Copolymers and Tacticity Control in Controlled/Living Radical Polymerization, *J. Am. Chem. Soc.*, 2003, **125**(23), 6986–6993, DOI: 10.1021/ja029517w.

11 K. Kempe, C. R. Becer and U. S. Schubert, Microwave-Assisted Polymerizations: Recent Status and Future Perspectives, *Macromolecules*, 2011, **44**(15), 5825–5842, DOI: 10.1021/ma2004794.

12 M. Chen, M. Zhong and J. A. Johnson, Light-Controlled Radical Polymerization: Mechanisms, Methods, and Applications, *Chem. Rev.*, 2016, **116**(17), 10167–10211, DOI: 10.1021/acs.chemrev.5b00671.

13 Y. Kojima, S. Koda and H. Nomura, Effect of Ultrasonic Frequency on Polymerization of Styrene under Sonication, *Ultrason. Sonochem.*, 2001, **8**(2), 75–79, DOI: 10.1016/S1350-4177(00)00064-X.

14 M. Tarnacka, A. Dzienia, P. Maksym, A. Talik, A. Zięba, R. Bielas, K. Kaminski and M. Paluch, Highly Efficient ROP Polymerization of ε-Caprolactone Catalyzed by Nanoporous Alumina Membranes. How the Confinement Affects the Progress and Product of ROP Reaction, *Macromolecules*, 2018, **51**(12), 4588–4597, DOI: 10.1021/acs.macromol.8b00409.

15 A. Dzienia, P. Maksym, M. Tarnacka, I. Grudzka-Flak, S. Golba, A. Zięba, K. Kaminski and M. Paluch, High Pressure Water-Initiated Ring Opening Polymerization for the Synthesis of Well-Defined α-Hydroxy-ω-(Carboxylic Acid) Polycaprolactones, *Green Chem.*, 2017, **19**(15), 3618–3627, DOI: 10.1039/C7GC01748K.

16 B. L. Buss and G. M. Miyake, Photoinduced Controlled Radical Polymerizations Performed in Flow: Methods, Products, and Opportunities, *Chem. Mater.*, 2018, **30**(12), 3931–3942, DOI: 10.1021/acs.chemmater.8b01359.

17 A. P. Chiriac and C. I. Simionescu, Magnetic Field Polymerisation, *Prog. Polym. Sci.*, 2000, **25**(2), 219–258, DOI: 10.1016/S0079-6700(99)00037-4.

18 A. M. Doerr, J. M. Burroughs, S. R. Gitter, X. Yang, A. J. Boydston and B. K. Long, Advances in Polymerizations Modulated by External Stimuli, *ACS Catal.*, 2020, **10**(24), 14457–14515 https://pubs.acs.org/doi/10.1021/acscatal.0c03802.

19 Q. Li, Z. Lu, H. Yang, J. Cai, X. Yin, Y. Zhao, L. Xiao and L. Hou, Photoinduced Organocatalyzed Controlled Radical Polymerization Feasible over a Wide Range of Wavelengths, *Polym. Chem.*, 2022, **13**, 527–535, DOI: 10.1039/D1PY01444G.

20 *Handbook of Radical Polymerization*, ed. K. Matyjaszewski and T. P. Davis, John Wiley & Sons, Inc., 2002, DOI: 10.1002/0471220450.

21 P. Maksym, R. Bernat, K. Koperwas, M. Wojtyniak, J. Piecha, B. Hachula, M. Geppert-Rybczynska, A. Brzozka, G. D. Sulka, M. Tarnacka, M. Paluch and K. Kaminski, The Unique Role of Pore Wall Nanostructurization in the Intrachannel Photo-ATRP for Fine-Tuning PMMA Tacticity,

Chem. Commun., 2022, **58**, 13015–13018, DOI: 10.1039/d2cc05250d.

22 P. Maksym, M. Tarnacka, R. Bernat, A. Dzienia, A. Szelwicka, B. Hachuła, A. Chrobok, M. Paluch and K. Kamiński, Light-Mediated Controlled and Classical Polymerizations of Less-Activated Monomers under High-Pressure Conditions, *Polym. Chem.*, 2021, **12**(30), 4418–4427, DOI: 10.1039/D1PY00738F.

23 P. Maksym, M. Tarnacka, A. Dzienia, K. Erfurt, A. Brzęczek-Szafran, A. Chrobok, A. Zięba, K. Kaminski and M. Paluch, High Pressure RAFT of Sterically Hindered Ionic Monomers. Studying Relationship between Rigidity of the Polymer Backbone and Conductivity, *Polymer*, 2018, **140**, 158–166, DOI: 10.1016/j.polymer.2018.02.030.

24 K. Chat, P. Maksym, K. Kaminski and K. Adrjanowicz, Stereoregulation, Molecular Weight, and Dispersity Control of PMMA Synthesized via Free-Radical Polymerization Supported by the External High Electric Field, *Chem. Commun.*, 2022, **58**(37), 5653–5656, DOI: 10.1039/D2CC01186G.

25 W. Tu, A. Dzienia, P. Maksym, D. M. Duarte, A. B. Unni, K. Chat, K. Kaminski and K. Adrjanowicz, Electric-Field Assisted Ring-Opening Polymerization: On the Kinetics and Product Properties of DGEBA/Aniline Model System, *Polymer*, 2022, **254**, 125085, DOI: 10.1016/j.polymer.2022.125085.

26 W. Tu, P. Maksym, K. Kaminski, K. Chat and K. Adrjanowicz, Free-Radical Polymerization of 2-Hydroxyethyl Methacrylate (HEMA) Supported by a High Electric Field, *Polym. Chem.*, 2022, **13**(19), 2850–2859, DOI: 10.1039/D2PY00320A.

27 D. Khandelwal, S. Hooda, A. S. Brar and R. Shankar, Stereoregularity Evolution of Isobornyl Acrylate and Styrene Copolymers by 2D NMR Spectroscopy, *J. Mol. Struct.*, 2013, **1049**, 99–111, DOI: 10.1016/J.MOLSTRUC.2013.05.046.

28 D. Khandelwal, S. Hooda and A. S. Brar, Configurational Sequence Determination of Poly(Isobornyl Acrylate) by NMR Spectroscopy, *J. Mol. Struct.*, 2011, **991**(1–3), 24–30, DOI: 10.1016/J.MOLSTRUC.2011.01.017.

29 K. B. Kockler, A. P. Haehnel, F. Fleischhaker, M. Schneider-Baumann, A. M. Misske and C. Barner-Kowollik, No Apparent Correlation of Kp with Steric Hindrance for Branched Acrylates, *Macromol. Chem. Phys.*, 2015, **216**(14), 1573–1582, DOI: 10.1002/MACP.201500140.

30 N. Heidarzadeh, E. G. Bygott and R. A. Hutchinson, Exploiting Addition–Fragmentation Reactions to Produce Low Dispersity Poly(Isobornyl Acrylate) and Blocky Copolymers by Semibatch Radical Polymerization, *Macromol. Rapid Commun.*, 2020, **41**(16), 2000288, DOI: 10.1002/MARC.202000288.

31 B. Dervaux, T. Junkers, M. Schneider-Baumann, F. E. du Prez and C. Barner-Kowollik, Propagation Rate Coefficients of Isobornyl Acrylate, Tert-Butyl Acrylate and 1-Ethoxyethyl Acrylate: A High Frequency PLP-SEC Study, *J. Polym. Sci., Part A: Polym. Chem.*, 2009, **47**(23), 6641–6654, DOI: 10.1002/POLA.23706.

32 K.-C. Cheng, Y.-Y. Su, T.-H. Chuang, W. Guo and W.-F. Su, Kinetic Model of Hyperbranched Polymers Formed by Self-Condensing Vinyl or Self-Condensing Ring-Opening Polymerization of AB Monomers Activated by Stimuli with Different Reactivities, *Macromolecules*, 2010, **43**, 8965–8970, DOI: 10.1021/ma101740r.

33 W. Jakubowski, A. Juhari, A. Best, K. Koynov, T. Pakula and K. Matyjaszewski, Comparison of Thermomechanical Properties of Statistical, Gradient and Block Copolymers of Isobornyl Acrylate and n-Butyl Acrylate with Various Acrylate Homopolymers, *Polymer*, 2008, **49**(6), 1567–1578, DOI: 10.1016/J.POLYMER.2008.01.047.

34 B. Dervaux, W. van Camp, L. van Renterghem and F. E. du Prez, Synthesis of Poly(Isobornyl Acrylate) Containing Copolymers by Atom Transfer Radical Polymerization, *J. Polym. Sci., Part A: Polym. Chem.*, 2008, **46**(5), 1649–1661, DOI: 10.1002/POLA.22505.

35 K. Matyjaszewski, The Synthesis of Functional Star Copolymers as an Illustration of the Importance of Controlling Polymer Structures in the Design of New Materials, *Polym. Int.*, 2003, **52**(10), 1559–1565, DOI: 10.1002/PI.1339.

36 D. R. D'hooge, M.-F.-O. Reyniers, F. J. Stadler, B. Dervaux, C. Bailly, F. E. Du Prez and G. B. Marin, Atom Transfer Radical Polymerization of Isobornyl Acrylate: A Kinetic Modeling Study, *Macromolecules*, 2010, **43**, 8766–8781, DOI: 10.1021/ma101736j.

37 E. E. Kulikov, S. D. Zaitsev and Y. D. Semchikov, Reversible Addition-Fragmentation Chain Transfer (RAFT) (Co) Polymerization of Isobornyl Acrylate, *Polym. Sci., Ser. C*, 2015, **57**(1), 120–127, DOI: 10.1134/S1811238215010051.

38 A. J. Back and F. J. Schork, Emulsion and Miniemulsion Polymerization of Isobornyl Acrylate, *J. Appl. Polym. Sci.*, 2007, **103**(2), 819–833, DOI: 10.1002/APP.25181.

39 T. Pirman, M. Ocepek and B. Likozar, Radical Polymerization of Acrylates, Methacrylates, and Styrene: Biobased Approaches, Mechanism, Kinetics, Secondary Reactions, and Modeling, *Ind. Eng. Chem. Res.*, 2021, **60**(26), 9347–9367, DOI: 10.1021/ACS.IECR.1C01649.

40 E. Van De Reydt, N. Marom, J. Saunderson, M. Boley and T. Junkers, A Predictive Machine-Learning Model for Propagation Rate Coefficients in Radical Polymerization, *Polym. Chem.*, 2023, **14**, 1622, DOI: 10.1039/d2py01531e.

41 D. Khandelwal, S. Hooda, A. S. Brar and R. Shankar, Poly (Isobornyl Methacrylate-Co-Methyl Acrylate): Synthesis and Stereosequence Distribution Analysis by NMR Spectroscopy, *J. Polym. Sci., Part A: Polym. Chem.*, 2012, **50**(16), 3350–3362, DOI: 10.1002/POLA.26122.

42 D. Khandelwal, S. Hooda, A. S. Brar and R. Shankar, Stereoregularity Evolution of Isobornyl Acrylate and Styrene Copolymers by 2D NMR Spectroscopy, *J. Mol. Struct.*, 2013, **1049**, 99–111, DOI: 10.1016/J.MOLSTRUC.2013.05.046.

43 S. Havriliak and S. Negami, A Complex Plane Representation of Dielectric and Mechanical Relaxation Processes in Some Polymers, *Polymer*, 1967, **8**(C), 161–210, DOI: 10.1016/0032-3861(67)90021-3.

44 H. Vogel, The Law of the Relation between the Viscosity of Liquids and the Temperature, *Phys. Z.*, 1921, **22**, 645–646.
45 G. S. Fulcher, Analysis of Recent Measurements of the Viscosity of Glasses, *J. Am. Ceram. Soc.*, 1925, **8**, 339–355, DOI: **10.1111/j.1151-2916.1992.tb05536.x**.
46 G. Tammann and W. Hesse, Die Abhängigkeit Der Viscosität von Der Temperatur Bie Unterkühlten Flüssigkeiten, *Z. Anorg. Allg. Chem.*, 1926, **156**(1), 245–257, DOI: **10.1002/zaac.19261560121**.
47 R. Böhmer, K. L. Ngai, C. A. Angell and D. J. Plazek, Nonexponential Relaxations in Strong and Fragile Glass Formers, *J. Chem. Phys.*, 1998, **99**(5), 4201, DOI: **10.1063/1.466117**.
48 S. Ozlem, E. Aslan-Gürel, R. M. Rossi and J. Hacaloglu, Thermal Degradation of Poly(Isobornyl Acrylate) and Its Copolymer with Poly(Methyl Methacrylate) via Pyrolysis Mass Spectrometry, *J. Anal. Appl. Pyrolysis*, 2013, **100**, 17–25, DOI: **10.1016/J.JAAP.2012.10.024**.
49 J. Brandrup, E. H. Immergut, E. A. Grulke, A. Abe, D. R. Bloch, J. Wlley, N. Y. Chichester, W. Brisbane and S. Toronto, *Polymer Handbook*, 1999.
50 T. G. Fox Jr. and P. J. Flory, Second–Order Transition Temperatures and Related Properties of Polystyrene. I. Influence of Molecular Weight, *J. Appl. Phys.*, 1950, **21**, 581–591.
51 R. Kohlrausch, Nachtrag Uber Die Elastische Nachwirkung Beim Cocon Und Glasfaden, *Ann. Phys.*, 1847, **12**(393), 393–399.
52 G. Williams and D. C. Watts, Non-Symmetrical Dielectric Relaxation Behaviour Arising from a Simple Empirical Decay Function, *Trans. Faraday Soc.*, 1970, **66**, 80–85, DOI: **10.1039/tf9706600080**.
53 K. Chat, W. Tu, A. Beena Unni and K. Adrjanowicz, Influence of Tacticity on the Glass-Transition Dynamics of Poly(Methyl Methacrylate) (PMMA) under Elevated Pressure and Geometrical Nanoconfinement, *Macromolecules*, 2021, **54**(18), 8526–8537, DOI: **10.1021/acs.macromol.1c01341**.